

RESEARCH

Open Access



# Assessment of muscle fiber types transformation in rats with discogenic low back pain using diffusion tensor image of paraspinal muscles

Ying Wu<sup>1</sup>, Jiyao Ma<sup>1</sup>, Yilong Huang<sup>1</sup>, Zhengguang Zhang<sup>1</sup>, Jiangyuan Pi<sup>2</sup>, Chao Gao<sup>1</sup>, Wenyang Leng<sup>1</sup> and Bo He<sup>1\*</sup>

## Abstract

**Background** The onset of discogenic lower back pain (DLBP) was strongly associated with fiber-type transformation in the paraspinal muscles. Management of DLBP would be greatly benefited from an objective, noninvasive biomarker for assessing fiber composition. Our study aimed to explore the value of diffusion tensor imaging (DTI) in evaluating fiber-type transformation, which contributed to improve diagnosis and intervention strategies on DLBP.

**Methods** According to time since model establishment, ninety healthy female Sprague Dawley rats were randomly divided into the 1st month group, 3rd month group, and 6th month group, then each group was subdivided into the DLBP group, sham-operated group, and control group. The L4/5 and L5/6 intervertebral discs of rats underwent posterior-entry puncture disruption and sham-operation to establish DLBP and sham-operation groups. DTI MRI and immunofluorescence (IF) were performed to assess fiber type transformation.

**Results** The DLBP rats exhibited a gradual decrease in Fractional Anisotropy (FA) values. At the 3rd month and 6th month after modeling, there was a significant decrease in the percentage of type I fiber, while an increase in the percentage of type II fiber. Notably, the percentage of type I fiber demonstrated a moderate positive correlation with FA values.

**Conclusion** DTI may serve as a potential tool to investigate the fiber type transformation in DLBP rats.

**Clinical trial number** Not applicable.

**Keywords** Diffusion tensor image, Discogenic low back pain, Muscle fiber type transformation, Rats

\*Correspondence:

Bo He

kmmu\_hb@163.com

<sup>1</sup>Department of Radiology, The First Affiliated Hospital of Kunming Medical University, Kunming, Yunnan, China

<sup>2</sup>Kunming Medical University, Kunming, Yunnan, China



© The Author(s) 2025. **Open Access** This article is licensed under a Creative Commons Attribution-NonCommercial-NoDerivatives 4.0 International License, which permits any non-commercial use, sharing, distribution and reproduction in any medium or format, as long as you give appropriate credit to the original author(s) and the source, provide a link to the Creative Commons licence, and indicate if you modified the licensed material. You do not have permission under this licence to share adapted material derived from this article or parts of it. The images or other third party material in this article are included in the article's Creative Commons licence, unless indicated otherwise in a credit line to the material. If material is not included in the article's Creative Commons licence and your intended use is not permitted by statutory regulation or exceeds the permitted use, you will need to obtain permission directly from the copyright holder. To view a copy of this licence, visit <http://creativecommons.org/licenses/by-nc-nd/4.0/>.

## Introduction

Discogenic low back pain (DLBP) is defined as a clinical disorder caused by disc pathology [1]. As the global population ages, DLBP will become a serious global health concern requiring immediate attention [2].

Studies have shown that the lumbar spine and structures surrounding it may be responsible for the occurrence of low back pain (LBP) [3]. The paravertebral muscles (lumbar multifidus and erector spinae) play an important role in spinal stability and function [4]. Proportional composition of fiber type determines the functions in muscles. The transformation in fiber type was assumed to be a possible factor in the etiology and recurrence of pain, as it negatively affected muscle strength and endurance [5]. Meanwhile, research has suggested that poor back muscle endurance in patients with LBP may be attributed to a higher proportion of type II fast-twitch fibers [6–7].

DLBP is the most common form of LBP, with a significant motor disability. Although studies have indicated that DLBP patients exhibited fiber type transformation in paraspinal muscles [8], not all studies have found the differences in fiber types between DLBP and healthy individuals. Therefore, little is known about the fiber type characteristics of paraspinal muscles in DLBP patients [9], it necessitates further investigation. However, there are significant obstacles in performing muscle biopsies in humans, with the lack of a reliable non-invasive tool being one of the major hindrances in evaluating fiber transformation in DLBP.

Diffusion tensor imaging (DTI) is sensitive to the random diffusion of water molecules within tissue, it used to detect white matter fiber tracts. Owing to the highly anisotropic of water molecules in muscle, DTI has been successfully applied to track fibers number and volume in calf muscles [10], and considered as a valuable tool to explore physiological and pathological alterations in skeletal muscle microstructure [11–12]. Berry et al. found that fiber size was closely related with minor eigenvalues, fractional anisotropy (FA) and mean diffusivity (MD) values [12]. Elisabeth et al. proposed that DTI may track subtle changes in back muscle composition that relate to muscle strength [13], and Scheel et al. found that DTI was a promising method to noninvasively estimate the fiber proportion in the calf muscles [14]. However, the ability of this method to characterize paraspinal muscle fiber types in patients with DLBP remains largely unknown.

The intervertebral disc (IVD) degeneration in rats have a similar cellular composition when compared to the human [15]. Our research utilizes the rat model to explore whether fiber type transformation occurs in DLBP and to evaluate the potential of DTI in assessing this process within paraspinal muscles.

## Methods

### Rats

This study was approved by animal experiment ethics committee (Kmmu20220762). The procedures were reported in compliance with the ARRIVE (Animal Research: Reporting of In Vivo Experiments) guidelines [16], all experiments used healthy adult female Sprague Dawley rats (220–250 g, about 4 weeks old upon arrival, animal license No.: SYXK(Dian)K2020-0006). The minimum sample size (90 rats) was calculated using PASS software (NCSS, USA). Prior to randomization into distinct groups, the animals were housed in standard chambers within an SPF laboratory animal room and allowed to adapt for 1 week.

### Experimental grouping

According to time since model establishment, ninety rats were randomly divided into the 1st month group, 3rd month group, and 6th month group, then each group was subdivided into the DLBP group, sham-operated group, and control group; there were nine groups in total ( $N = 10/\text{group}$ ). The age/size/weight/holding conditions of all rats were matched.

### DLBP model

The DLBP models were established according to a method described in previous study [17]. The rats were completely anesthetized by intraperitoneal injection of sodium pentobarbital (30 mg/kg), and under fluoroscopic guidance, the L4/5 and L5/6 intervertebral discs in rats were disrupted via injection of phosphate-buffered saline (60  $\mu\text{L}$ ) using disposable puncture needles (width 25G, length 20 mm) to establish DLBP model, successful modeling was confirmed by nucleus pulposus signal reduction on T2WI MRI and behavioral experiments. To control for the impact of the puncture procedure on the paravertebral muscles, sham-operated rats underwent skin and muscle perforation at the L4/5 and L5/6 levels without inducing disc damage, while the DLBP group received full disc injury. Control group without any treatment. The overall study design was shown in Fig. 1.

### Behavioral experiments

Following successful modeling in rats, all rats were subjected to tail suspension test, grasping test, wire hang test, four limb grip strength test, and forced swimming test. The study measured lower back pain severity and paravertebral muscle function.

### Tail suspension test (TST)

The TST was carried out according to Can et al. [18]. Over a period of five minutes, three people recorded the duration of the rat's struggling, bending, and immobility, with each observer assigned to one specific behavior.

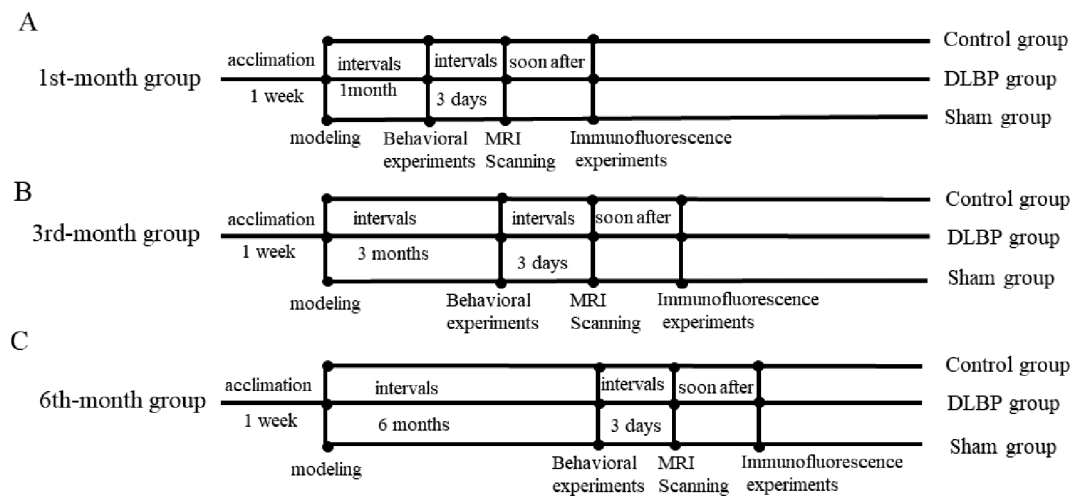


**Fig. 1** Schematic of experimental design. **(A)** Experimental Procedures in the 1st-month group; **(B)** Experimental Procedures in the 3rd-month group; **(C)** Experimental Procedures in the 6th-month group

**Table 1** The specific imaging protocols

Sequences	TR (ms)	TE (ms)	NEX	Slice thickness (mm)	Bandwidth (MHz)	FOV (cm×cm)	SNR	Pixel size(m)	Slice gap
Sagittal T2WI	3610.0	120.0	2.0	1.2	31.25	10.0×10.0	58	0.3×0.4	0
Axial MENSA	36.4	6.6	0.78	1.0	31.25	8.0×8.0	45	0.3×0.3	0
Coronal MUSE-DTI	7000.0	74	2.0	1.0	166.7	10.0×10.0	25	1.0×1.0	0

### Grasping test

The Grasping Test was carried out according to Dai et al. [19]. Rats were placed on an iron grid, which was inverted on a glass cylinder that was 35 cm high, and the time from when they grasped the grid until they fell onto the ground was recorded (Upper limit:20s).

### Wire hang test

The Wire Hang Test was carried out according to Kada et al. [20]. A wire was attached to two vertical sticks, and a soft mattress was placed underneath to cushion the rats' fall. The rats were enticed to grasp the wire, and the longest time (in seconds) they stayed on it before falling was recorded.

### Four limb grip strength test

The Four Limb Grip Strength Test was carried out according to van et al. [21]. We connected a metal grid horizontally to a tensiometer (WDF-10, Wenzhou Weidu Electronic Co., LTD, Wenzhou, China). The rats were allowed to grip the grid horizontally with four limbs. We gently held the mid-tail of a rat and slowly pulled it out of the grid until the rat let go. The maximum grasping force (N) was recorded.

### Forced swimming test

The Forced Swimming Test was carried out according to Arauchi et al. [22]. Rats were placed in a glass cylinder (diameter = 25 cm; height = 50 cm) containing warm

water ( $25 \pm 1^\circ\text{C}$ ) at a depth of 40 cm; and an object was dangled from its tail, the rats were allowed to swim freely in the cylinder. When the rat's snout was submerged underwater for 5 s and prevented from resurfacing, the latency to exhaustion was recorded.

### MRI scanning and post-processing

On the 3rd-day, following the behavioral experiments, we injected all rats with sodium pentobarbital (30 mg/kg) for intraperitoneal anesthesia, the paraspinal muscles at the L4/5 and L5/6 levels of all rats were scanned with a 3.0 T whole-body system (Signa™Architect 3.0T, GE Healthcare, Boston, USA) using the 16-channel rat-specific coil (CG-MUC49-H300-AG, Shanghai Chenguang Medical Technologies Co., LTD, Shanghai, China).DTI sequence with fat suppression(Spectral Presaturation with Inversion Recovery, SPIR), the diffusion time was 12min40s. The specific imaging protocols were shown in Table 1. For DTI data processing, we used the commercial software called Volume Viewer (14.0 Ext.8) in post-processing workstation (Advantage Windows 4.6, GE Medical Systems, USA). The regions of interest (ROIs) were manually drawn along the contours of the multifidus and the erector spinae, while avoiding the fasciae and the surrounding inter-muscular adipose tissue.

### Immunofluorescence

Following the DTI scan, all rats were anesthetized with overdose of sodium pentobarbitone(50 mg/kg). At the

L4/5 and L5/6 levels in rats, bilateral multifidus and erector spinae were biopsied, and cut into 5  $\mu\text{m}$  sections with a paraffin slicer (Leica Biosystems, Shanghai, China). After sealing with 3% BSA, it was dripped with primary antibody: MYH1(catalog #:gb112130; Servicebio; Wuhan, China) and MYH7(catalog #:gb112131; Servicebio; Wuhan, China), and then incubated overnight at 4 °C refrigerator; subsequently, we dripped the second antibody: (catalog #: A11005; Invitrogen; shanghai, China) and (catalog #: A11008; Invitrogen; shanghai, China). Finally, images were photographed under a fluorescence microscope (CM1950, Olympus, Tokyo, Japan), and the percentage of type I and type II muscle fiber were measured according to the fluorescence intensity, and the mean fiber diameters were counted using ImageJ (NIH, MD) under 20 $\times$ objective. Percentage of type I muscle fibers = type I fibers/(type I fibers + type II fibers)  $\times$  100%; percentage of type II muscle fibers = type II fibers/ (type I fibers + type II fibers)  $\times$  100%.

### Statistical analysis

All statistical analyses were performed using SPSS software (version 21.0; SPSS Inc, Chicago, IL, USA). All tests were done using a two-sided  $P < 0.05$  level of significance.

Normally distributed data was expressed as means  $\pm$  standard deviation (SD), One-way ANOVA was used to calculate the statistical significance between groups. If the normality assumption had not been met, the Kruskal-Wallis test was employed to assess statistical significance between groups. The Bonferroni correction test was applied for multiple comparison testing. Spearman correlation coefficients were calculated between the DTI parameters (FA, MD,  $\lambda_1$ ,  $\lambda_2$ ,  $\lambda_3$ ), mean fiber diameter, and the percentage of type I muscle fibers. Graphs were generated using GraphPad Prism software (version 9.0; GraphPad Software, San Diego, CA).

## Results

### Degree of pain in rats

**Tail suspension test.** At the 3rd and 6th months after modeling, immobility time and bending time in the DLBP group exhibited a gradual increase compared to other groups, while struggle time showed a significant decrease (all  $P < 0.05$ , Fig. 2A-C).

**Grasping test.** When compared to other groups, DLBP group demonstrated shorter durations, the most noticeable reduction at the 6th month (all  $P < 0.05$ , Fig. 2D).

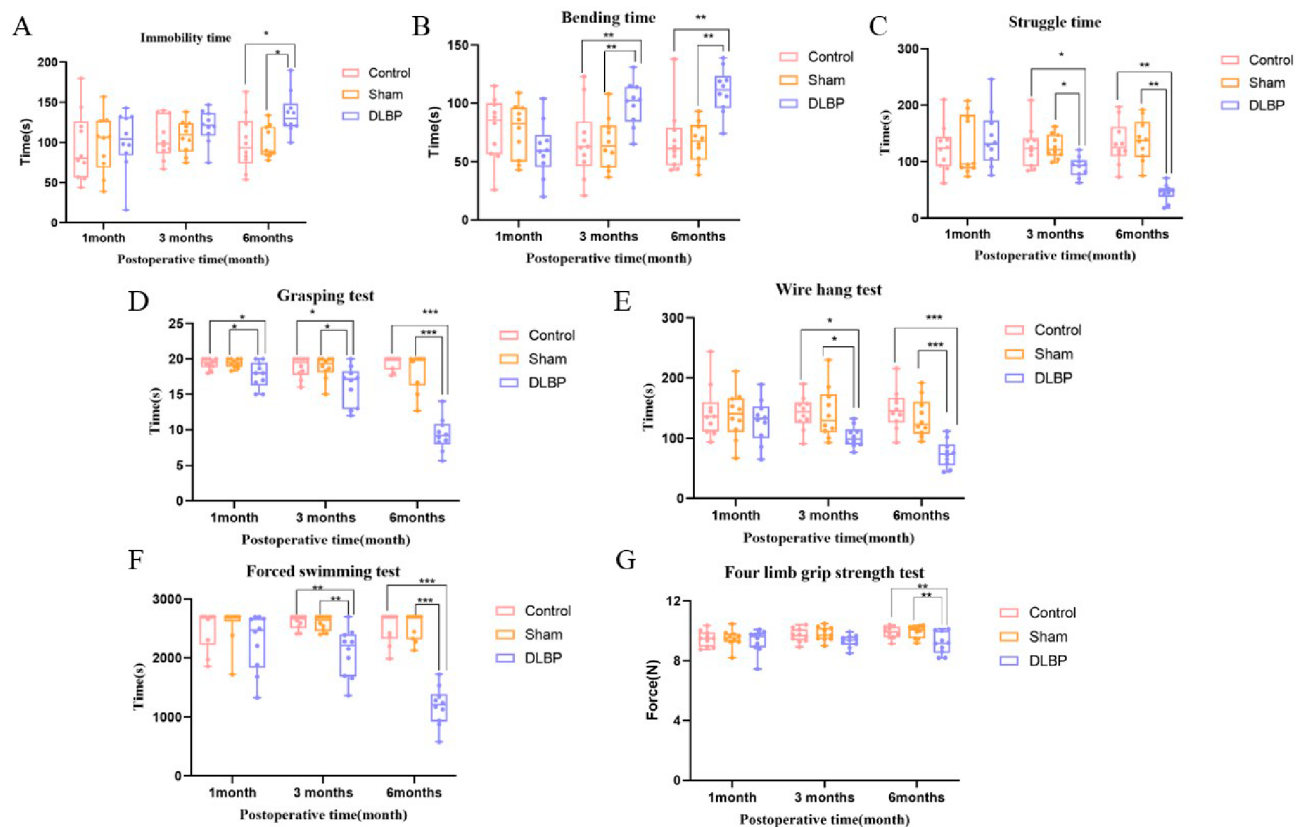


**Fig. 2** Results of behavioral experiments in rats. (A) Immobility time of rats in Tail suspension test. (B) Bending time of rats in Tail suspension test. (C) Struggle time of rats in Tail suspension test. (D) Grasping test. (E) Wire hang test. (F) Forced swimming test. (G) Four limb grip strength test. Data were presented as means  $\pm$  standard deviation. \* $P < 0.05$ , \*\* $P < 0.01$ , \*\*\* $P < 0.001$

### Paravertebral muscle endurance in rats

Wire hang test. At the 3rd and 6th months after modeling, when compared to other groups, the maximum duration in DLBP group was progressively decreased (all  $P < 0.05$ , Fig. 2E).

Forced swimming test. At the 3rd and 6th months after modeling, compared to other groups, the DLBP group exhibited a gradual reduction in time to exhaustion. The most notable reduction occurred at the 6th month after modeling ( $P < 0.001$ ; Fig. 2F).

### Paravertebral muscle strength in rats

Four limb grip strength test. when compared to other groups, four-limb grip strength in DLBP group was significantly decrease at the 6th month after modeling ( $P < 0.01$ ; Fig. 2G).

### DTI parameters analysis

At the 6th month after modeling, compared to other groups, the DLBP group exhibited significantly decreased FA values in the multifidus and erector spinae muscles ( $P < 0.01$ ; Fig. 3A), while MD values were significantly increased ( $P < 0.05$ ; Fig. 3B). FA and MD parameter maps were shown (Fig. 4A, B).

For the  $\lambda_1$  values, there were no significant differences in any group ( $P > 0.05$ ; Fig. 5A); but for  $\lambda_2$  and  $\lambda_3$  values, the DLBP group exhibited significant increases compared to the sham-operated and control groups at 6th months after modeling ( $P < 0.05$ ; Fig. 5B, C).

### Percentage of muscle fibers and mean fiber diameter in rat

At 3rd and 6th months after modeling, the DLBP group exhibited a significant decrease in the percentage of type I muscle fibers and an increase in type II muscle fibers compared to other groups, with the most notable increase observed at 6th months after modeling ( $P < 0.05$ ; Fig. 6A), but for the mean fiber diameter, there were no statistically differences in any group ( $P > 0.05$ ; Fig. 6B).

### Correlation between DTI and the percentage of type I fibers

The correlations of DTI parameters with the percentages of type I fibers in the multifidus muscle and erector spinae muscles are presented in Table 2. The results showed that the percentage of type I fiber demonstrated a moderate positive correlation with FA, and was weakly negatively correlated with MD and  $\lambda_3$ .

### Correlation between DTI parameters and the mean fiber diameter

The correlations of DTI parameters with the mean fiber diameter in the multifidus muscle and erector spinae are presented in Table 3. The results showed that the mean fiber diameter was not correlated significantly with DTI parameters ( $P > 0.05$ ).

### Discussion

In the DLBP rats, we observed a decrease in FA values, and an increase in MD and  $\lambda_3$  values. Meanwhile, there was a significant decrease in the percentage of type I

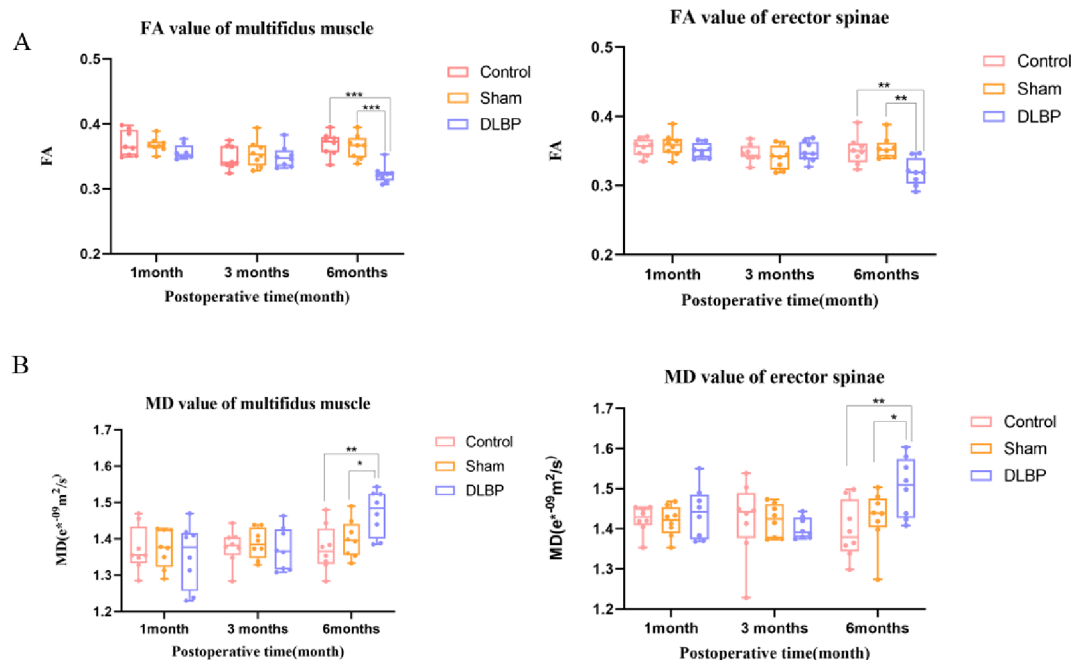


**Fig. 3** FA and MD values of paravertebral muscles in rats at different time. (A) FA values in the multifidus and erector spinae. (B) MD values in the multifidus and erector spinae. Data were presented as means  $\pm$  standard deviation. \* $P < 0.05$ , \*\* $P < 0.01$ , \*\*\* $P < 0.001$



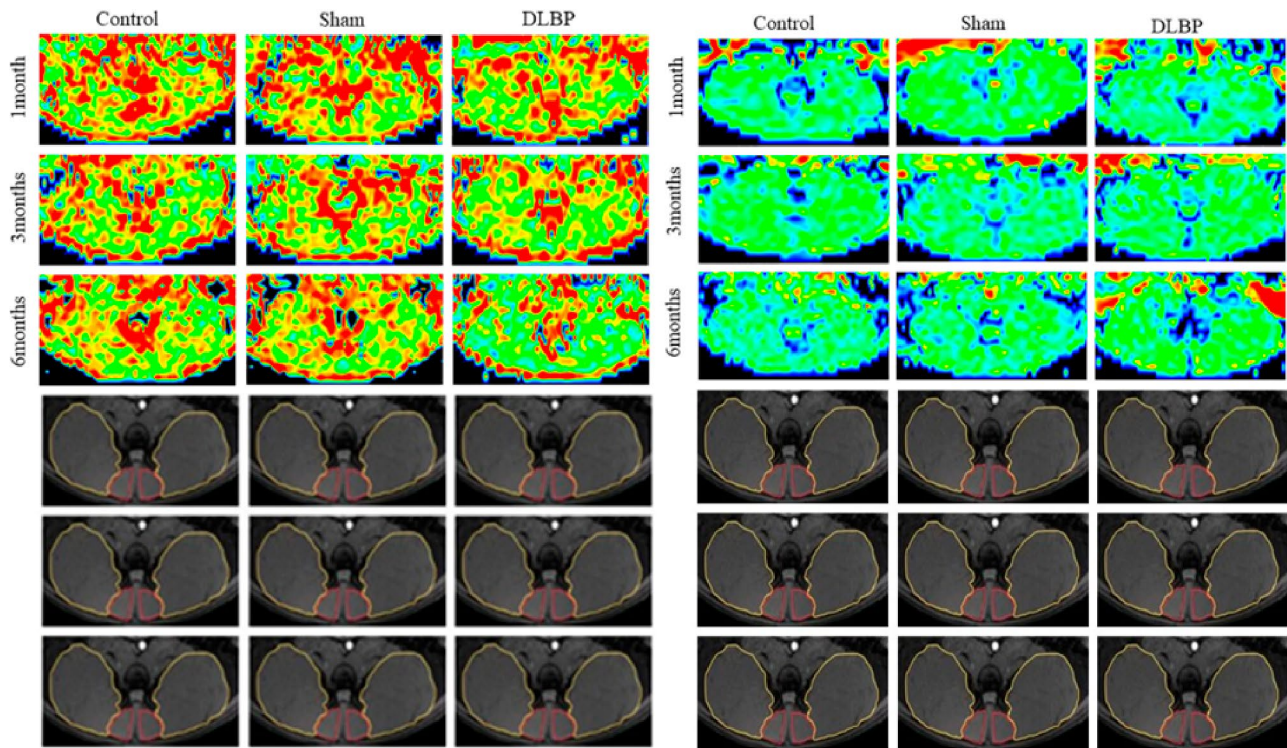


**Fig. 4** FA and MD maps of paravertebral muscles in rats at different time. **(A)** FA parameters maps in the multifidus and erector spinae. **(B)** MD parameters maps in the multifidus and erector spinae. **(C)** Anatomical image in the paravertebral muscles as reference for the ROIs align with the maps. (Red circles indicate the multifidus muscle and orange circles indicate the erector spinae in anatomical image; In muscle parameter maps, the blue-green-yellow-red color gradient indicates a progression from low to high values in both FA and MD)

fibers, whereas the percentage of type II fibers increased. Furthermore, the percentage of type I fibers demonstrated a positive correlation with FA.

Animal models play a crucial role in elucidating disease mechanisms and exploring candidate therapies, thus, we established rat model to gain deeper insights into DLBP. Clinically, the degree of DLBP was assessed by asking for medical history and using various pain scoring scales [23], but it was not suitable for rats. We observed the behavior in rats [24–26], and revealed that rats with DLBP exhibited increased pathological severity, accompanied by reduced endurance and compromised fatigue resistance in the paravertebral muscles.

Paravertebral core stability disorder was an important factor in the occurrence of LBP [27], and to meet the stability demands, different back muscles fiber played different roles. In humans, skeletal muscle fibers are classified into two main types: Type I slow-twitch oxidative fibers (Type I) and Type II fast-twitch glycolytic fibers (Type II). Type I fibers demonstrate significantly higher endurance and fatigue resistance compared to Type II fibers, which makes them particularly advantageous for sustaining postural control. However, it was unclear whether the fiber-type transition rendered these patients more susceptible to developing DLBP or whether changes in fiber type occurred as a consequence of DLBP. Pakzad et

al. proposed that dysfunctional pain may lead to change in fiber types in LBP patients [28], which was consistent with our findings. But our results about fiber transformation in DLBP rats was inconsistent with Agten et al. [7], firstly, specific etiologies can cause morphological changes, they studied non-specific chronic low back pain (NSCLBP) patients, whose etiology was frequently unknown. Secondly, they only biopsied paravertebral fiber at single L4 level, and macro characteristics of the muscle were not analyzed. For these reasons and others, it necessitates further investigation to clarify this hypothesis.

We systematically reviewed previous research showing that DTI parameters are influenced by the microstructure and pathological changes of tissues: (1) The type and organelle density of fiber. In general, Type II muscle fibers exhibit lower mitochondrial density and reduced myoglobin concentration compared to Type I fibers, consequently enabling water molecules within the muscle tissue to undergo more facile diffusion, the observed microstructural changes resulted in significantly increased MD and decreased FA; (2) Mechanical overload and inflammation. These factors could lead to fiber remodeling and adaptation to the altered mechanical demands. In the acute stage, due to the inflammatory response, which caused cell swelling and an increase in

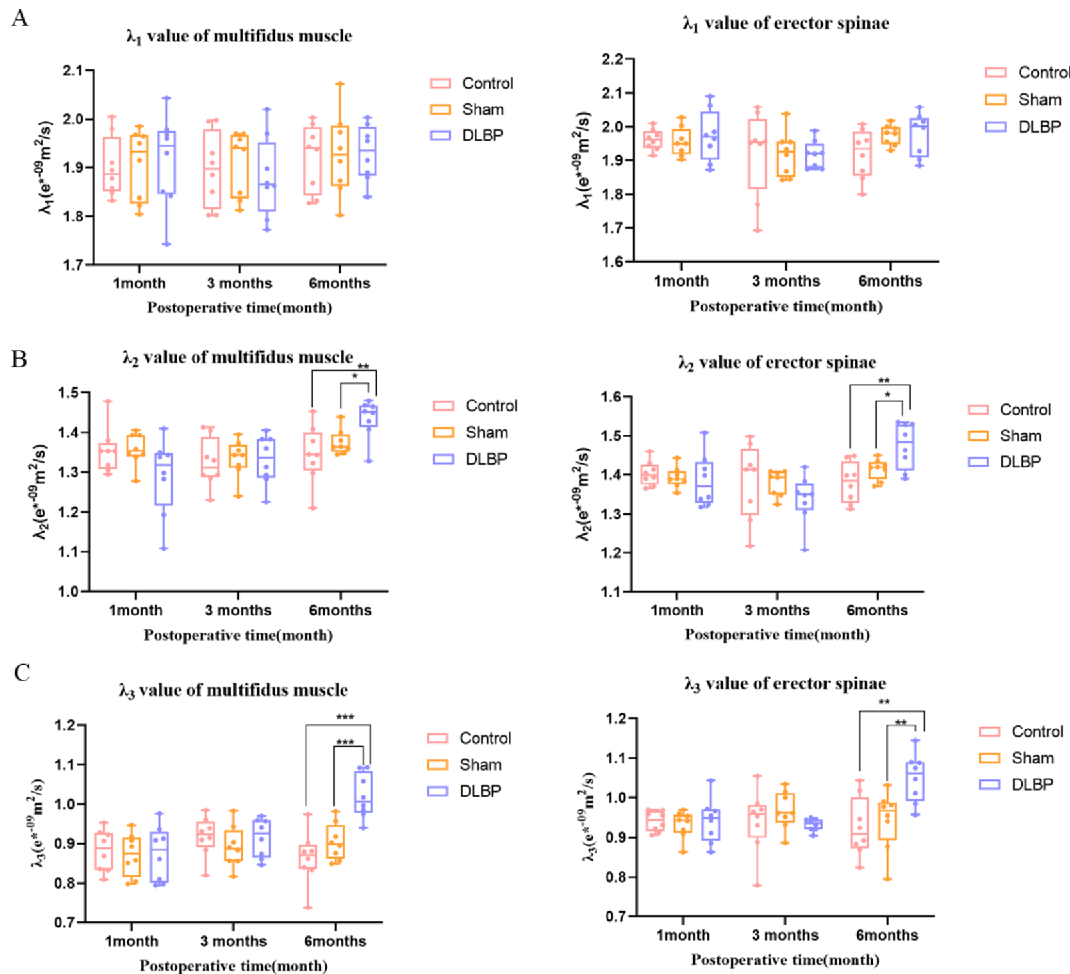


**Fig. 5**  $\lambda_1$ ,  $\lambda_2$ , and  $\lambda_3$  values of paravertebral muscles in rats at different time. **(A)**  $\lambda_1$  values in the multifidus and erector spinae. **(B)**  $\lambda_2$  values in the multifidus and erector spinae. **(C)**  $\lambda_3$  values in the multifidus and erector spinae. Data were presented as mean  $\pm$  standard deviation. \* $P < 0.05$ , \*\* $P < 0.01$ , \*\*\* $P < 0.001$

extracellular fluid, there was a decrease in FA and an increase in MD [29]. (3) Neural and hormonal factors. Studies found the decline in growth hormone secretion may contribute to a reduction in the number of type II fibers and fiber diameters; consequently, the reduction in fiber diameter could affect diffusion microenvironment [30]. Denervation serves as the primary instigator of severely atrophic fiber accumulation. This structural degeneration induces compartmental shrinkage, resulting in decreased MD and increased FA due to enhanced diffusion directionality constraints [31].

Based on our findings, a similar observation was confirmed by Scheel et al. [14]. When synthesized with prior evidence, the phenotypic transform from type I to type II muscle fibers reduces interstitial space volume and diminishes tissue anisotropy. These microstructural alterations consequently decrease FA while elevating MD and radial eigenvalues ( $\lambda_2$ ,  $\lambda_3$ ), reflecting enhanced isotropic water diffusion.

The lack of correlation between mean fiber diameter and DTI parameters indicates that fiber size is unlikely to dominantly regulate extracellular diffusion dynamics. In DLBP rats, type II fibers demonstrated a significantly higher proportion compared to type I fibers, thus the cross-sectional area occupied by type II fibers exceeded that of type I fibers. Berry et al. proposed that DTI as a sensitive tool to monitor muscle atrophy by measuring fiber size [32], and the mean fiber diameter was no statistically differences in any group. However, no significant muscle atrophy was observed in our DLBP rats, consequently, additional ultrastructural details of type I fibers that impact on diffusion should be explored.

To control for the impact of the puncture procedure on the paravertebral muscles, sham-operated rats underwent skin and muscle perforation at the L4/5 and L5/6 levels without inducing disc damage, while the DLBP group received full disc injury. In our results, the sham-operation group showed the same functional effect as the control group, while showed the different effects from

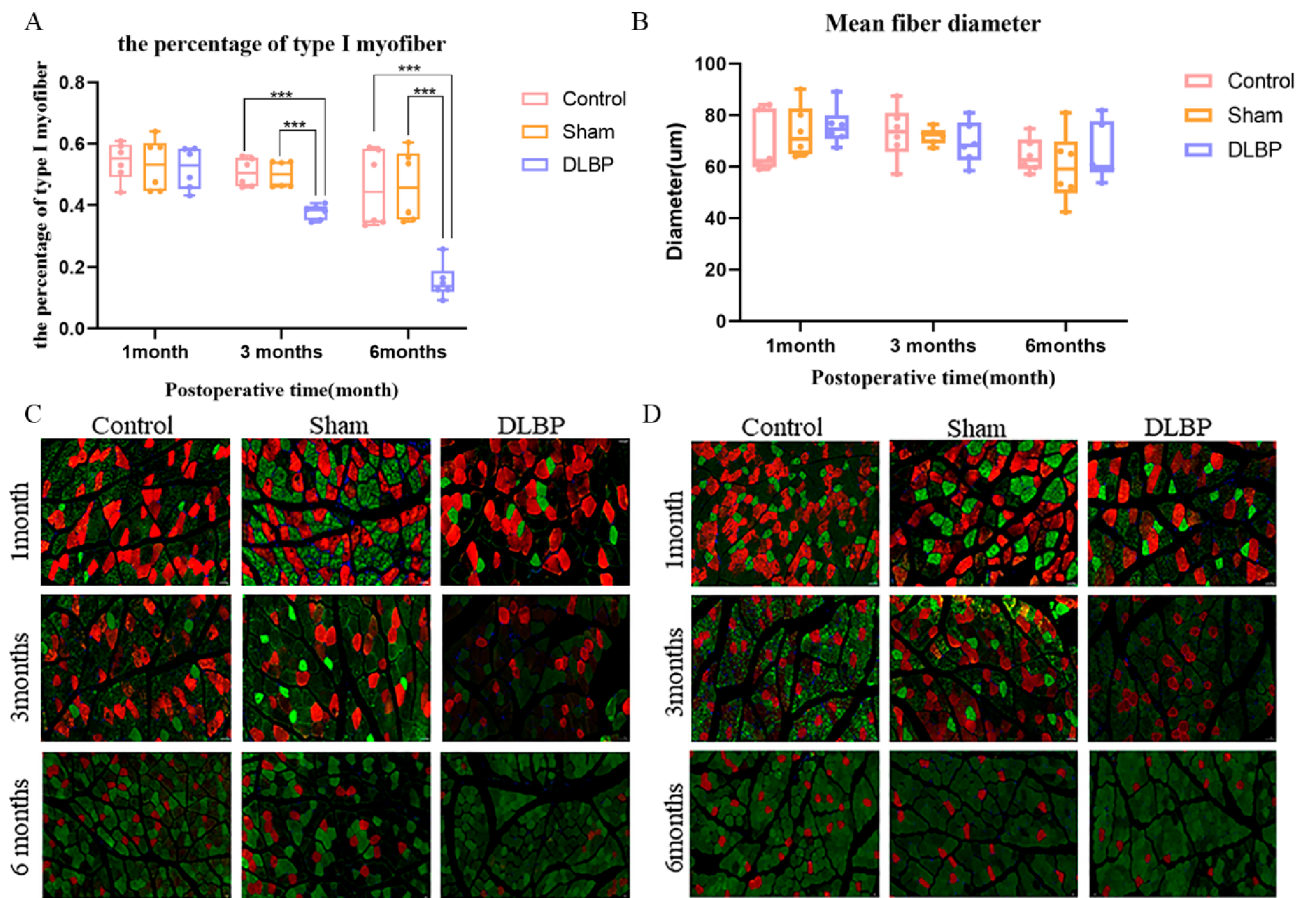


**Fig. 6** Immunofluorescence of paravertebral muscles in rats at different time (200× magnification). **(A)** Percentage of type I fiber in rats. **(B)** Mean fiber diameter in rats. **(C)** Immunofluorescence image in multifidus muscle. **(D)** Immunofluorescence image in erector spinae. Data were presented as mean ± standard deviation. \* $P < 0.05$ , \*\* $P < 0.01$ , \*\*\* $P < 0.001$ . (In the immunofluorescence images: red indicates the type I fiber, and green indicates the type II fiber)

**Table 2** Correlation between DTI parameters and the percentage of type I myofiber

		FA	MD	$\lambda_1$	$\lambda_2$	$\lambda_3$
I%	r	0.493***	-0.273*	-0.143	-0.253	-0.397*
	p	< 0.001	0.046	0.304	0.065	0.003

I%, the percentage of type I myofiber

**Table 3** Correlation between DTI parameters and the mean fiber diameter

DTI parameter	Mean ± standard deviation	Correlation with mean fiber diameter(r/p)
FA	0.36 ± 0.02	-0.216/0.116
MD	1.40 ± 0.06	-0.023/0.868
$\lambda_1$	1.92 ± 0.08	-0.104/0.455
$\lambda_2$	1.37 ± 0.06	-0.100/0.470
$\lambda_3$	0.93 ± 0.06	0.075/0.590

DLBP groups, findings that confirm our hypothesis that demonstrated fiber-type transition in the paravertebral muscles of DLBP rats.

Huang et al. showed that significant fatty infiltration of the paraspinal muscles at the L4-L5 and L5-S1 levels in patients with DLBP. This finding implies that fatty infiltration in paraspinal muscles might emerge as a diagnostic biomarker for managing DLBP [17]. Regarding the etiology of fatty infiltration in paraspinal muscles, Chen et al. proposed that there was a moderately positive relationship between fatty infiltration within the vertebral body and that in the multifidus muscle in patients with LBP, highlighting the need for longitudinal studies to establish causality [33]. Current literature on lumbar degenerative diseases predominantly centers on the multifidus muscle,



particularly its association with spinal stability. In contrast, the potential involvement of the erector spinae, especially regarding its fatty infiltration patterns, has yet to be systematically examined. Eksi et al. found that fatty infiltration in the erector spinae, especially at the upper lumbar spine level, may serve as a potential biomarker for LBP [34]. It was also observed that a higher degree of fatty infiltration in the erector spinae was associated with an increased likelihood of requiring surgical intervention in patients with lumbar spondylolisthesis [35]. The association between fatty infiltration in the paraspinal muscles and LBP requires further investigation.

There were several limitations in the current study. Firstly, we did not explore the underlying mechanisms responsible for the observed muscle fiber type transformation. Secondly, there were species differences between rats and humans, therefore, our results need to be further confirmed by clinical trials.

## Conclusion

In rats with DLBP, a transform from type I to type II muscle fibers was observed in the paravertebral muscles, most prominently at the 6th month after the onset of LBP, and the percentage of type I fiber was positive correlation with FA. DTI may serve as a potential tool to investigate the fiber type transformation in DLBP rats.

## Abbreviations

DLBP	Discogenic lower back pain
LBP	Low back pain
DTI	Diffusion tensor imaging
IF	Immunofluorescence
FA	Fractional Anisotropy
MD	Mean diffusivity
IVD	Intervertebral disc
SE-EPI	Spin-echo planar imaging
SNR	Signal-to-noise ratio

## Acknowledgements

Not applicable.

## Author contributions

BH proved final approval of the version. YH made Conception and design. JM, ZZ made literature research. CG made Experimental studies/data analysis. JP made Interpretation of data. WL made manuscript preparation. YW made manuscript editing.

## Funding

This work was supported by the National Natural Science Foundation of China (82260338), Yunnan Provincial Fundamental Research Projects (202201AC070669, 202201AU070051, 202301AS070016), and Yunnan Provincial Basic Research Program-Provincial and University Joint Special Project(202301AY070001-114).

## Data availability

The datasets used and/or analysed during the current study are available from the corresponding author on reasonable request.

## Declarations

### Ethical approval

This study was approved by animal experiment ethics committee (Kmmu20220762).

### Consent to participate

Not applicable.

### Consent to publish

Not applicable.

### Institutional licensing statement

All rats were purchased from the Animal Testing Center of the Faculty of Experimental Animals, Kunming Medical University. The license number is SYXK(Dian)K2020-0006.

### All methods were carried out in accordance with relevant guidelines and regulations

All applicable international, methods, and/or institutional guidelines for the care and use of animals were followed. The experiments were carried out in compliance with the guidelines of the National Research Council's Guide for the Care and Use of Laboratory Animals. All the procedures were reported in compliance with the ARRIVE (Animal Research: Reporting of In Vivo Experiments) guidelines.

### Competing interests

The authors declare no competing interests.

Received: 6 November 2024 / Accepted: 5 May 2025

Published online: 21 May 2025

## References

1. Takahashi M, Iwamoto K, Kuzuyama M, et al. Incidence of spinal instability among patients with discogenic low back pain with different backgrounds. *J Phys Ther Sci*. 2021;33:601–5.
2. Geurts JW, Willems PC, Kallewaard JW, van Kleef M, Dirksen C. The impact of chronic discogenic low back pain: costs and patients' burden. *Pain Res Manag*. 2018;2018:4696180.
3. Wang X, Jia R, Li J, et al. Research progress on the mechanism of lumbarmultifidus injury and degeneration. *Oxid Med Cell Longev*. 2021;2021:6629037.
4. Hodges PW, Danneels L. Changes in structure and function of the back muscles in low back pain: different time points, observations, and mechanisms. *J Orthop Sports Phys Therapy*. 2019;49:464–76.
5. Cagnie B, Dhooge F, Schumacher C, et al. Fiber typing of the erector spinae and multifidus muscles in healthy controls and back pain patients: A systematic literature review. *J Manipulative Physiol Ther*. 2015;38:653–63.
6. LariviÈre C, Da Silva RA, Arsenault AB, Nadeau S, Plamondon A, Vadeboncoeur R. Specificity of a back muscle exercise machine in healthy and low back pain subjects. *Med Sci Sports Exerc*. 2010;42:592–9.
7. Talbot J, Maves L. Skeletal muscle fiber type: using insights from muscle developmental biology to dissect targets for susceptibility and resistance to muscle disease. *Wires Dev Biol*. 2016;5:518–34.
8. Jones GE, Kumbhare DA, Harish S, Noseworthy MD. Quantitative DTI assessment in human lumbar stabilization muscles at 3 T. *J Comput Assist Tomogr*. 2013;37:98–104.
9. Noonan AM, Brown SHM. Paraspinal muscle pathophysiology associated with low back pain and spine degenerative disorders. *Jor Spine*. 2021;4.
10. Giraudo C, Motyka S, Weber M, Feiweier T, Trattng S, Bogner W. Diffusion tensor imaging of healthy skeletal muscles. *Invest Radiol*. 2019;54:48–54.
11. Bruschetta D, Anastasi G, Andronaco V, et al. Human calf muscles changes after strength training as revealed by diffusion tensor imaging. *J Sports Med Phys Fit*. 2019;59:853–60.
12. Martin-Noguerol T, Barousse R, Wessell DE, Rossi I, Luna A. A handbook for beginners in skeletal muscle diffusion tensor imaging: Physical basis and technical adjustments. *Eur Radiol*. 2022;32:7623–31.
13. Klupp E, Cervantes B, Schlaeger S, et al. Paraspinal muscle DTI metrics predict muscle strength. *J Magn Reson Imaging*. 2019;50:816–23.
14. Scheel M, von Roth P, Winkler T, et al. Fiber type characterization in skeletal muscle by diffusion tensor imaging. *NMR Biomed*. 2013;26:1220–4.

15. Diwan AD, Melrose J. Intervertebral disc degeneration and how it leads to low back pain. *Jor Spine*. 2022;6.
16. Boutron I, Percie du Sert N, Hurst V, et al. The ARRIVE guidelines 2.0: Updated guidelines for reporting animal research. *PLoS Biol*. 2020;18.
17. Huang Y, Wang L, Luo B, et al. Associations of lumbar disc degeneration with paraspinal muscles myosteatosis in discogenic low back pain. *Front Endocrinol (Lausanne)*. 2022;13:891088.
18. Can A, Dao DT, Terrillion CE, Piantadosi SC, Bhat S, Gould TD. The tail suspension test. *J Vis Exp*. 2012;e3769.
19. Dai C, Liu Y, Dong Z. Tanoshine I alleviates motor and cognitive impairments via suppressing oxidative stress in the neonatal rats after hypoxic-ischemic brain damage. *Mol Brain*. 2017;10:52.
20. Kada Sanda A, Nantia AE, Manfo TFP, et al. Subchronic administration of Parastar insecticide induced behavioral changes and impaired motor coordination in male Wistar rats. *Drug Chem Toxicol*. 2020;45:426–34.
21. van Putten M, Kumar D, Hulsker M, et al. Comparison of skeletal muscle pathology and motor function of dystrophin and utrophin deficient mouse strains. *Neuromuscul Disord*. 2012;22:406–17.
22. Arauchi R, Hashioka S, Tsuchie K, et al. Gunn rats with glial activation in the hippocampus show prolonged immobility time in the forced swimming test and tail suspension test. *Brain Behav*. 2018;8:e01028.
23. Inoue G, Kaito T, Matsuyama Y, et al. Comparison of the effectiveness of Pharmacological treatments for patients with chronic low back pain: A nationwide, multicenter study in Japan. *Spine Surg Relat Res*. 2021;5:252–63.
24. Millecamps M, Czerminski JT, Mathieu AP, Stone LS. Behavioral signs of axial low back pain and motor impairment correlate with the severity of intervertebral disc degeneration in a mouse model. *Spine J*. 2015;15:2524–37.
25. Millecamps M, Tajerian M, Sage EH, Stone LS. Behavioral signs of chronic back pain in the SPARC-null mouse. *Spine (Phila Pa 1976)*. 2011;36:95–102.
26. Wei S, Geng X, Li Z, et al. A forced swim-based rat model of premenstrual depression: Effects of hormonal changes and drug intervention. *Aging*. 2020;12:24357–70.
27. Quittner M, Rantalainen T, Ridgers ND, et al. Intervertebral disc status is associated with vertebral marrow adipose tissue and muscular endurance. *Eur Spine J*. 2018;27:1704–11.
28. Pakzad M, Fung J, Preuss R. Pain catastrophizing and trunk muscle activation during walking in patients with chronic low back pain. *Gait Posture*. 2016;49:73–7.
29. Tan ET, Zochowski KC, Sneag DB. Diffusion MRI fiber diameter for muscle denervation assessment. *Quant Imaging Med Surg*. 2022;12:80–94.
30. Hennessey JV, Chromiak JA, DellaVentura S, et al. Growth hormone administration and exercise effects on muscle fiber type and diameter in moderately frail older people. *J Am Geriatr Soc*. 2001;49:852–8.
31. Otto LAM, van der Pol WL, Schlaffke L, et al. Quantitative MRI of skeletal muscle in a cross-sectional cohort of patients with spinal muscular atrophy types 2 and 3. *NMR Biomed*. 2020;33.
32. Berry DB, Regner B, Galinsky V, Ward SR, Frank LR. Relationships between tissue microstructure and the diffusion tensor in simulated skeletal muscle. *Magn Reson Med*. 2017;80:317–29.
33. Chen J, Huang Y, Yang Y, et al. Vertebral bone quality score was associated with paraspinal muscles fat infiltration, but not modic classification in patients with chronic low back pain: a prospective cross-sectional study. *BMC Musculoskelet Disord*. 2024;25(1):509.
34. Ekşi MŞ, Özcan-Ekşi EE. Fatty infiltration of the erector spinae at the upper lumbar spine could be a landmark for low back pain. *Pain Pract*. 2024;24(2):278–87.
35. Ekşi MŞ, Öztaş UO, Topaloğlu F, et al. Erector spinae could be the game changer in surgical decision-making in patients with lumbar spondylolisthesis: a cross-sectional analysis of an age-, sex-, subtype-, level-matched patients with similar spinopelvic parameters received surgical or conservative management. *Eur Spine J*. 2024;33(10):3715–23.

## Publisher's note

Springer Nature remains neutral with regard to jurisdictional claims in published maps and institutional affiliations.